

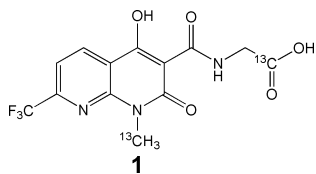
## Different Modes of Inhibitor Binding to Prolyl Hydroxylase by Combined Use of X-ray Crystallography and NMR Spectroscopy of Paramagnetic Complexes

Leszek Poppe,<sup>\*,†</sup> Christopher M. Tegley,<sup>§</sup> Vivian Li,<sup>†</sup> Jeffrey Lewis,<sup>‡</sup> James Zondlo,<sup>‡</sup> Evelyn Yang,<sup>‡</sup> Robert JM Kurzeja,<sup>‡</sup> and Rashid Syed<sup>†</sup>

Department of Molecular Structure, Protein Science, Chemistry Research and Discovery, Amgen, Inc., Thousand Oaks, California 91320

Received September 18, 2009; E-mail: lpoppe@amgen.com

Prolyl-4-hydroxylase (PHD2) is one of three known 2-oxoglutarate, Fe(II)-dependent oxygenases, which by regulating the hypoxia-inducible transcription factor (HIF) play an important role in oxygen homeostasis in humans.<sup>1</sup> Small molecule inhibition of PHD2, which mainly down-regulates the hypoxic response in normoxia, has been intensely pursued for the possible treatment of anemia and ischemic disease.<sup>2</sup> Insights into the development of PHD2 inhibitors have been gained from crystal structures of the C-terminal catalytic domain in complex with isoquinoline<sup>3</sup> or azaquinolone (**1**)-type compounds. In contrast to crystallographic data, in solution, **1** binds to PHD2 in a bimodal fashion. Here we present a strategy which utilizes the paramagnetic properties of a complexed metal ion<sup>4</sup> and requires introduction of only a few isotopic labels into the protein (<sup>15</sup>N) and into an inhibitor (<sup>13</sup>C), which, in conjunction with the crystallographic data, allowed us, in a quick and cost-effective way, to obtain both complex structures of **1**.



For NMR spectroscopy, homogeneous protein samples are required, yet both expression and purification steps yielded highly heterogeneous mixtures of *apo* and multiple *holo* forms of the protein. Inductively coupled plasma (ICP) analyses of different protein samples showed the presence of iron, zinc, and nickel or cobalt, picked from the purification columns. Consequently, all NMR samples were prepared by first completely removing all the divalent metal ions from the protein and then stoichiometrically adding a single metal ion: Fe<sup>2+</sup>, Co<sup>2+</sup>, or Zn<sup>2+</sup> and an inhibitor. Although the nickel ion has the highest affinity (Table S1), it turned out to be the least useful in obtaining structural information (*vide infra*).

All the *holo* forms of PHD2 have the divalent metal ion complexed in the same octahedral configuration.<sup>3</sup> In the X-ray structure compound **1** coordinates the metal ion via amide carbonyl and phenolic oxygens. The appearance of two distinct signals in <sup>19</sup>F spectra of **1** (Figure S1) demonstrates two binding modes of the inhibitor in the solution state. To gain more structural information, we introduced two additional <sup>13</sup>C spin labels into the N-methyl and carboxylic groups of the **1**. The <sup>13</sup>C spectra (Figure S2) show that, in one orientation of the ligand, the N-methyl group experi-

ences pronounced paramagnetic relaxation resulting from the close proximity (<5 Å) to the metal center. Since chemical shifts for the carbonyl resonances in both diamagnetic complexes are almost degenerate and indicate the same hydrogen bond with Arg383,<sup>3</sup> it is conceivable that the alternative complex has the same crystallographic position but the quinoline ring is flipped by 180° around the C(ring)–C(amide) bond. To further test this hypothesis in a more quantitative way, we analyzed <sup>19</sup>F and <sup>13</sup>C paramagnetic shifts in terms of two different orientations of the ligand, the crystallographic (“X”) and the flipped (“F”) one. The integrations of NMR signals from both complexes showed 2:1 (Fe<sup>2+</sup>) and 3:2 (Co<sup>2+</sup>, Ni<sup>2+</sup>, and Zn<sup>2+</sup>) ratios in favor of the “X” complex.

Since the molar ratio of both forms is similar for the different *holo* forms of the protein we assumed, in analogy to the Ratio Method,<sup>5</sup> that the *relative* spin delocalization mechanism is identical for the different metal ions. Thus, for a particular ligand nucleus, the ratios of the contact shifts between two different conformations should be the same for the different metal ions. In the case of iron and cobalt complexes this may be expressed by the following equation:

$$\frac{\delta_{X,Fe(II)}^p - \delta_{X,Fe(II)}^{PCS}}{\delta_{F,Fe(II)}^p - \delta_{F,Fe(II)}^{PCS}} = \frac{\delta_{X,Co(II)}^p - \delta_{X,Co(II)}^{PCS}}{\delta_{F,Co(II)}^p - \delta_{F,Co(II)}^{PCS}} \quad (1)$$

which for the two nuclei case is equivalent to the Ratio Method (eqs 4–14 of ref 5). The  $\delta^p$  and  $\delta^{PCS}$  symbols correspond to the observed paramagnetic and pseudocontact shifts respectively.

The subscripts designate ligand conformation and metal ion. To use this equation for optimizing ligand positions, magnetic susceptibility tensors for both metal ions and both ligand conformations must be known. These tensors were obtained from protein samples with <sup>15</sup>N labeled tryptophans.<sup>6</sup> Figure 1 shows the overlay of <sup>15</sup>N–<sup>1</sup>H HSQC spectra for [<sup>15</sup>N-Trp]-PHD2(Co<sup>2+</sup>) and [<sup>15</sup>N-Trp]-PHD2(Zn<sup>2+</sup>) complexed with **1**. The observed doubling of peaks originates from two different magnetic susceptibility tensors corresponding to the “X” and “F” orientation of the ligand. These tensors, for the Fe(II) and Co(II) complexes, were calculated from the PCSs (Figure 1) and crystallographic coordinates for the protein (Table 2S). In the case of nickel, the pseudocontact shifts were too small for accurate determination of the tensor. Thus, the nickel complex was not included in the analysis.

The results of the optimizations based on eq 1 (see SI for the details) are listed in Table 1. The calculations separated the paramagnetic shifts for the ligand into pseudocontact and contact contributions. With regard to the structures of the two complexes, the calculated rmsd values are very small and indicate that “X” and “F” conformations (Figure S3) are the only possible solutions. Similar results were obtained with the Ratio Method,<sup>5</sup> assuming

<sup>†</sup> Department of Molecular Structure.

<sup>§</sup> Chemistry Research and Discovery.

<sup>‡</sup> Protein Science.

**Table 1.** Analysis of Paramagnetic Shifts for **1** Complexed to PHD2 in Two Different Orientations and in the Presence of Different Metal Ions

complex type:		ligand in "X" position			ligand in "F" position		
shifts/ppm	metal ion	CF <sub>3</sub>	CH <sub>3</sub>	CO	CF <sub>3</sub>	CH <sub>3</sub>	CO
paramagnetic (experimental) <sup>a</sup>	Fe <sup>2+</sup>	-2.8	1.5	5.1	2.2	17.3	7.1
	Co <sup>2+</sup>	6.9	7.4	-24.2	5.05	51.1	-22.8
	Ni <sup>2+</sup>	0.65	0.5	-3.5	-0.65	19.9	-3.5
pseudocontact <sup>b</sup>	Fe <sup>2+</sup>	-1.05 ± 0.3	10.6 ± 1	4 ± 0.5	0.6 ± 0.25	-18.8 ± 4.4	5.5 ± 0.7
	Co <sup>2+</sup>	6.8 ± 0.2	10.7 ± 1	-22.5 ± 1.9	5.1 ± 0.2	38 ± 3.5	-20.5 ± 2.2
contact	Fe <sup>2+</sup>	-1.8 ± 0.3	-9.1 ± 1	1.1 ± 0.5	1.6 ± 0.2	36.2 ± 4.5	1.6 ± 0.7
	Co <sup>2+</sup>	0.1 ± 0.2	-3.3 ± 1	-1.7 ± 2	-0.1 ± 0.2	13.1 ± 3.4	-2.3 ± 2.2
rmsd <sup>c</sup>			0.1 ± 0.05 Å			0.1 ± 0.1 Å	

<sup>a</sup> <sup>19</sup>F and <sup>13</sup>C paramagnetic shifts in **1** complexed with different *holo* forms of the catalytic domain of PHD2. The experimental paramagnetic shifts were obtained from the differences of the corresponding chemical shifts for the paramagnetic complexes (Fe<sup>2+</sup>, Co<sup>2+</sup>, Ni<sup>2+</sup>) and the diamagnetic complex with Zn<sup>2+</sup>. The measurement error is less than 0.15 ppm. <sup>b</sup> The separation of the paramagnetic shifts into the pseudocontact and contact contributions was based on eq 1. The pseudocontact shifts were calculated from the magnetic susceptibility tensors obtained from the HSQC spectra of [<sup>15</sup>N-Trp]-PHD2 samples (SI Table S2). <sup>c</sup> Corresponds to rmsd values between the optimized and the crystallographic "X" or the flipped "F" positions of the ligand (Figure S3).

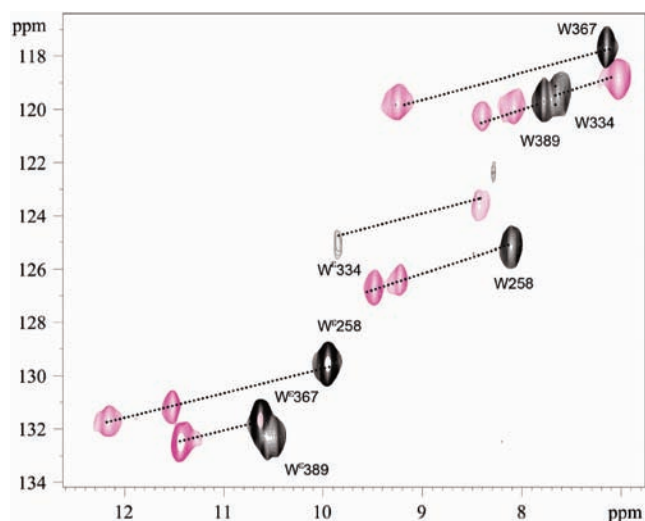


**Figure 1.** <sup>15</sup>N-<sup>1</sup>H HSQC spectrum of [<sup>15</sup>N-Trp]-PHD2<sub>173-403</sub> in complex with **1** and Zn<sup>2+</sup> (black) or Co<sup>2+</sup> (magenta). The cross-peaks corresponding to the same tryptophan residue in both spectra are connected with the dotted line. Spectral assignments were obtained from the magnetic susceptibility tensor calculations (Supporting Information (SI)).

identical ratios of contact shifts for each system differing only in the metal ion (data not shown). However, only in the case of assumptions underlying eq 1, the calculated contact shifts are consistent with the observed paramagnetic shifts for the nickel complex (Table 1), which are predominantly contact in nature.

Interestingly, the contact shifts are significantly larger in the case of the ferrous complex, which represents a more efficient mechanism of electron delocalization in this case, and are consistent with quantum mechanical calculations for the effects of iron substitution by cobalt or nickel in prolyl hydroxylases.<sup>8</sup>

In summary, we have demonstrated how NMR spectroscopy of paramagnetic complexes can complement crystallographic studies and enhance structure-based design efforts with respect to inhibitors for prolyl hydroxylases. As described, the NMR methodology efficiently extended the scope of the crystallographic method into the solution state where the azaquinolone inhibitors bind simulta-

neously in two different orientations. The knowledge of the alternative ligand orientation in the solution state opened new avenues for inhibitor design.

Although, in this case, the complexity of the system rendered its own solution, the simplified approach, where the contact contributions to the paramagnetic shifts could be neglected, allowed the determination of complex structures with a number of inhibitors for which no crystals were obtained. For these studies, cobalt complexes appeared to be superior to ferrous complexes due to the larger anisotropy of the magnetic susceptibility tensors and resilience to oxidation.

**Acknowledgment.** We would like to thank Jinshu Qiu for performing the ICP analyses.

**Supporting Information Available:** Protocols for protein expression, purification and metal removal, synthesis of <sup>13</sup>C labeled **1**; Experimental and computational details; Calorimetric affinities of different metal ions; <sup>19</sup>F and <sup>13</sup>C spectra of **1** in complexes; magnetic susceptibility tensors and numerical values for the experimental and calculated PCSs for the Fe<sup>2+</sup> and Co<sup>2+</sup> complexes. Complete ref 3. This material is available free of charge via Internet at <http://pubs.acs.org>.

## References

- (1) Schofield, Ch. J.; Ratcliffe, P. J. *Nat. Rev. Mol. Cell Biol.* **2004**, *40*, 343–354.
- (2) (a) Berra, E.; Benizri, A. G.; Ginouvès, A.; Volmat, V.; Roux, D.; Pousségur, J. *EMBO J.* **2003**, *22* (16), 4082–4090. (b) Hewitson, K. S.; Schofield, C. J. *Drug Discovery Today* **2004**, *9* (16), 704–711.
- (3) McDonough, J.; et al. *Proc. Natl. Acad. Sci.U.S.A.* **2006**, *103* (26), 9814–9819.
- (4) (a) Bertini, I.; Luchinat, C.; Parigi, G. *Prog. Nucl. Magn. Reson. Spectrosc.* **2002**, *40*, 249–273. (b) Pintacuda, G.; Keniry, M. A.; Huber, T.; Park, A. Y.; Dixon, N. E.; Otting, G. *J. Am. Chem. Soc.* **2004**, *126*, 2963–2970. (c) Zhuang, T.; Leffler, H.; Prestegard, J. H. *Protein Sci.* **2008**, *17* (7), 1220–1231.
- (5) Horrocks, W. DeW. In *NMR of Paramagnetic Molecules. Principles and Applications*; La Mar, G. N., Horrocks, W. DeW., Holm, R. H., Eds.; Academic Press: 1973.
- (6) Strauss, A.; Bitsch, F.; Cutting, B.; Fendrich, G.; Graff, P.; Liebetanz, J.; Zurini, M.; Jahnke, W. *J. Biomol. NMR* **2003**, *26*, 367–372.
- (7) Donaire, A.; Salgado, J.; Moratal, J. M. *Biochemistry* **1998**, *37*, 8659–8673.
- (8) Topol, I. A.; Nemukhin, A. V.; Salnokow, K.; Cachau, R. E.; Abashin, Y. G.; Kasprzak, K. S.; Burt, S. K. *J. Phys. Chem. A* **2006**, *110*, 4223–4228.

JA907933P